geosciences

MDPI

Article

An Exploratory GIS-Based Contribution to Geothermal Favourability Mapping in Hercynian Granite-Hosted Fractured Systems: Guarda District, Central Portugal

Vanessa Gonçalves [1], Leonardo Marchiori [1,*], Maria Vitoria Morais [1], Luís M. Ferreira Gomes [1], António Albuquerque [1], Pedro Gabriel Almeida [1], Hugo Alexandre Silva Pinto [1,2] and Luís José Andrade Pais [1]

[1] GeoBioTec, Civil Engineering Department, University of Beira Interior, 6201-001 Covilhã, Portugal; alvane.goncalves@ubi.pt (V.G.); vitoria.morais@ubi.pt (M.V.M.); lmfg@ubi.pt (L.M.F.G.); antonio.albuquerque@ubi.pt (A.A.); galmeida@ubi.pt (P.G.A.); hpinto@ubi.pt or hugopinto@ipg.pt (H.A.S.P.); ljap@ubi.pt (L.J.A.P.)

[2] School of Technology and Management, Department of Civil Engineering, Polytechnic Institute of Guarda, 6300-559 Guarda, Portugal

* Correspondence: leonardo.marchiori@ubi.pt

Abstract

Geothermal energy is a locally available, low-carbon resource that may support heat supply, building decarbonisation and regional energy diversification in non-volcanic crystalline settings. This study proposes an exploratory GIS-based approach for geothermal favourability mapping in the Guarda District, Central Portugal, where Hercynian granites, major fault systems and thermal and mineral water occurrences define a structurally controlled hydrogeothermal framework. Hydrogeochemical data from 54 groundwater abstraction points were integrated through silica-derived apparent geothermometric indicators, classical hydrothermal-parameter estimation and Empirical Bayesian Kriging Regression Prediction (EBKRP). Apparent silica-derived temperature indicators, circulation depth, geothermal gradient and theoretical thermal power were estimated, with $\log_{10}$ transformed thermal power used as the dependent variable and distance to major mapped faults as the structural covariate. Apparent silica-derived temperature indicators range from 21.3 °C to 121.2 °C, with a mean of 64.6 °C, while estimated geothermal gradients range from 20.3 °C/km to 92.1 °C/km. Higher estimated values occur preferentially near NE–SW and NNW–SSE fault systems, suggesting that structural permeability may influence deep groundwater circulation. The interpretation explicitly acknowledges that, in low-temperature systems, dissolved silica may be influenced by chalcedony or amorphous silica control, as well as by cooling, mixing and incomplete re-equilibration during fluid ascent. The resulting map is interpreted as a screening-level favourability product, not as a definitive assessment of exploitable geothermal resources, and supports the prioritisation of future structural mapping, geophysical surveys, exploratory drilling, borehole temperature logging and applied geothermal assessment in fractured granitic terrains.

Keywords: geothermal energy; geothermal favourability; fractured Hercynian granites; geographic information systems; Empirical Bayesian Kriging Regression Prediction; low- to medium-enthalpy resources; Guarda District

Academic Editors: John McBride and Gianluca Groppelli

Received: 18 May 2026
Revised: 26 June 2026
Accepted: 29 June 2026
Published: 2 July 2026

1. Introduction

Geothermal energy is widely recognised as a renewable resource with social, environmental and energy-security relevance [1]. Although its exploitation has traditionally been associated with volcanic or high-enthalpy settings, non-volcanic crystalline terrains may also host low- to medium-enthalpy hydrothermal systems, particularly where groundwater circulation is controlled by faults, fractures and deep structural discontinuities [2–4]. Recent studies from fractured granitic and crystalline basement terrains in southwest China, Taiwan and Central Europe have further demonstrated the scientific and applied relevance of these systems in non-volcanic crustal settings [5–8].

On the global scale, geothermal electricity production remains concentrated in a limited number of countries, which account for more than 80% of the installed capacity [9,10], estimated at approximately 16.2 GW across nearly 480 power plants [11]. In low- to medium-enthalpy systems, however, geothermal exploitation is commonly more suited to direct uses, including heating, building heating and cooling, and other thermal applications, thereby avoiding the conversion losses associated with electricity generation [12].

In non-volcanic crystalline regions, reservoirs with temperatures between approximately 20 °C and 100 °C may support direct applications such as district heating, building heating and cooling, balneotherapy, greenhouse heating, aquaculture and low-temperature industrial processes [12–17]. The Lindal diagram provides a reference framework for linking geothermal fluid temperature to suitable uses [17], while cascade utilisation allows the same resource to be exploited sequentially at decreasing temperature levels, increasing overall system efficiency [18] (Figure 1). Coupling these systems with geothermal heat pumps and closed-loop configurations may further enhance the use of moderate-temperature resources, particularly in decentralised heating and cooling solutions for buildings and agricultural facilities [19–21].

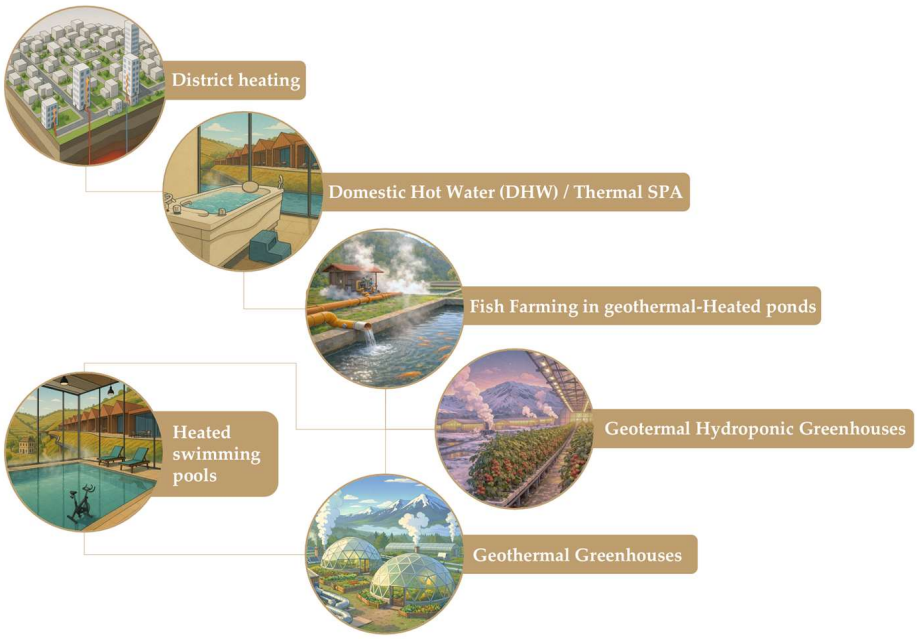

Figure 1. Conceptual scheme of cascade utilisation for geothermal fluids below 100 °C, illustrating sequential direct-use applications at decreasing temperature levels, adapted from Ferreira Gomes (2007) [22].

Portuguese geothermal resources are characterised by a clear contrast between insular volcanic settings, where high-enthalpy systems occur, and the mainland, where low- to medium-enthalpy hydrothermal systems predominate [18,23–26]. On the mainland, these

systems are mainly associated with deep groundwater circulation along late Hercynian fault systems [18,27]. The national geothermal inventory identifies approximately 61 geothermal and thermal occurrences in Portugal, mainly in the northern and central regions, associated with NE–SW and NNW–SSE fault systems [28]. Examples such as Chaves and São Pedro do Sul demonstrate the feasibility of low- to medium-enthalpy resources for balneotherapy, building heating and cooling, and other hydrothermal uses [18,29–31].

The Guarda District, dominated by Hercynian granitic rocks and hydrothermal manifestations such as Longroiva, Manteigas, Cró and Almeida [32–34], provides a favourable geological and hydrogeological setting for deep groundwater circulation within fractured massifs and granite–metasedimentary contacts. Although local deep borehole data are scarce, the possibility of locally enhanced geothermal gradients is supported by complementary evidence, including the national geothermal inventory [28], the spatial association between thermal waters and major faults [18,32], previous estimates for the district [33] and regional deep borehole data [35].

Low-enthalpy geothermal energy has gained increasing relevance in national energy and climate policy frameworks, particularly due to its potential contribution to decarbonisation, efficient heating and cooling, and district heating networks [36,37]. This strategic context, reinforced by the Strategic Plan for Geothermal Energy [28] and European funding mechanisms [38], supports the relevance of geothermal favourability mapping in the Guarda District as a tool for regional energy planning.

The present study develops an exploratory GIS-based approach to geothermal favourability mapping in the Guarda District, integrating silica-derived apparent geothermometric indicators, hydrothermal-parameter estimation and Empirical Bayesian Kriging Regression Prediction (EBKRP). The proposed workflow aims to estimate apparent hydrogeothermal screening indicators, assess their spatial relationship with major mapped fault systems and generate a preliminary favourability map to support the identification of priority areas for future geothermal exploration, validation and applied assessment in fractured granitic terrains.

2. Theoretical Background and State of Knowledge

2.1. Operational Temperature and Enthalpy Framework Adopted in This Study

The classification of geothermal systems according to reservoir temperature or enthalpy provides an operational criterion for assessing geothermal favourability and guiding potential uses, ranging from heating and cooling applications to direct uses and, under suitable conditions, electricity generation [39,40].

In non-volcanic crystalline environments, such as Hercynian granitic massifs, low primary permeability means that groundwater circulation is largely controlled by fractures, faults and weathered zones. Structural connectivity, continuity at depth, recharge conditions and the balance between conductive and convective heat transfer influence reservoir temperature and thermal productivity, as demonstrated from pioneering hot dry rock studies [41] to recent investigations of fractured granitic systems [7,8,42,43]. Deep faults may therefore act as preferential pathways for hydrothermal circulation and exert major control on the spatial distribution of thermal anomalies [44,45].

In this study, the temperature and enthalpy classification is used only as an operational framework for interpreting the results, following criteria applied in geothermal literature and Portuguese geothermal studies [22,39,46], although some variability in threshold values is acknowledged, including the approximate 25 °C limit for very low-enthalpy systems [39]. Table 1 provides a framework for assessing the potential applicability of the estimated values. The >100 °C class indicates higher relative thermal potential but does not imply direct feasibility for conventional electricity generation, which is generally associated

with temperatures ≥ 150 °C. Possible binary-cycle applications depend on discharge rate, reinjection conditions, conversion efficiency and economic viability [15,47–49].

Table 1. Operational classification of geothermal systems adopted in this study, based on reservoir temperature and potential applications, adapted from Ferreira Gomes (2007) [22] and Dickson and Fanelli (2003) [39].

Category Adopted in This Study	Temperature Range	Main Potential Applications
Higher relative thermal potential	>100 °C	Direct uses and, only under favourable flow-rate, reinjection, technological and economic conditions, possible future techno-economic assessment
Low- to medium-enthalpy	20–100 °C	Direct uses, including district heating, thermal bathing, aquaculture, agriculture, industry and building heating/cooling
Very low enthalpy	<20 °C	Shallow geothermal systems and building heating/cooling applications

2.2. Exploration Methods and GIS-Based Geothermal Favourability Assessment

Geothermal favourability assessment in non-volcanic crystalline terrains requires the integration of geological and structural information with hydrogeochemical, geophysical and geospatial data [50–53].

Hydrogeochemical methods are useful for deriving apparent silica-based geothermometric indicators and for inferring mixing, recharge and circulation processes in hydrothermal systems [54–57]. However, in fractured granitic aquifers, flow heterogeneity, variable residence times and mixing with meteoric waters may reduce the reliability of silica geothermometers and ionic equilibrium indicators [50,54,55,58]. Such estimates should therefore be interpreted as preliminary hydrogeochemical indicators and integrated with structural, geophysical and hydrogeological information [59]. In this context, silica-based estimates are used as comparative indicators of water–rock interaction and possible circulation depth, rather than as definitive evidence of equilibrium with a specific silica polymorph. In Portuguese granitic and sulphurous-water systems, silica geothermometry has been applied as a regional comparative tool since the pioneering work of Aires-Barros (1979) [60], and later in studies addressing alkaline sulphurous waters and granitic hydrogeothermal systems, including Calado (2001) [61], Morais (2013) [62] and Ferreira Gomes et al. (2015) [63].

Arnórsson (2000) [64] emphasised that the applicability of silica geothermometers depends on the temperature range, mineral equilibrium conditions and hydrogeochemical evolution of geothermal fluids. In low-temperature systems, dissolved silica may be controlled by chalcedony or amorphous silica rather than quartz equilibrium, and temperature estimates may be affected by dilution, cooling and mixing processes. Consequently, silica-derived temperatures should be evaluated together with the geological and hydrogeological context and interpreted with caution where thermodynamic equilibrium cannot be demonstrated. In regional-scale exploratory studies, silica geothermometers may nevertheless provide useful comparative indicators of relative hydrothermal circulation intensity and water–rock interaction processes. Geophysical methods complement geothermal assessment by characterising subsurface structure, fault continuity, fractured domains, conductive zones and thermal regimes at depth, providing an important basis for validating areas of predicted hydrothermal favourability [44,50,53].

Geographic Information Systems support geothermal assessment by integrating geological, structural, hydrogeochemical, thermal and geophysical data within a spatial framework [64–68]. These approaches commonly use interpolation, geostatistical mod-

elling and multicriteria analysis based on variables such as geothermal gradient, fault proximity, transmissivity, lithology, heat flow and geomorphological conditions [69–71]. In this study, EBKRP was adopted as an exploratory screening method because it combines regression, spatial prediction, explanatory covariates and uncertainty assessment [71–74]. Fault proximity was used as a structural covariate to predict theoretical thermal power in fractured granitic terrains. The resulting map expresses relative geothermal favourability, not recoverable resources, and should therefore be interpreted as a preliminary spatial model constrained by limited subsurface information [75].

3. Study Area

3.1. Geographic and Geomorphological Settings

The Guarda District in Central Portugal has a strongly contrasted geomorphological setting, with elevations ranging from approximately 101.5 m to 1991.9 m and culminating in the Serra da Estrela, the highest mountain range in mainland Portugal (Figure 2). This altitudinal gradient defines a compartmentalised landscape of mountains, plateaus and structural valleys, influencing surface runoff, recharge, infiltration and regional groundwater circulation. The Serra da Estrela and Serra da Marofa represent important recharge sectors, where high elevation and reactivated late Hercynian structures favour infiltration and deep circulation. Incised valleys may act as preferential discharge zones, while the contrast between smoother eastern landforms and more structurally controlled western plateaus influences secondary permeability and deep groundwater flow [76].

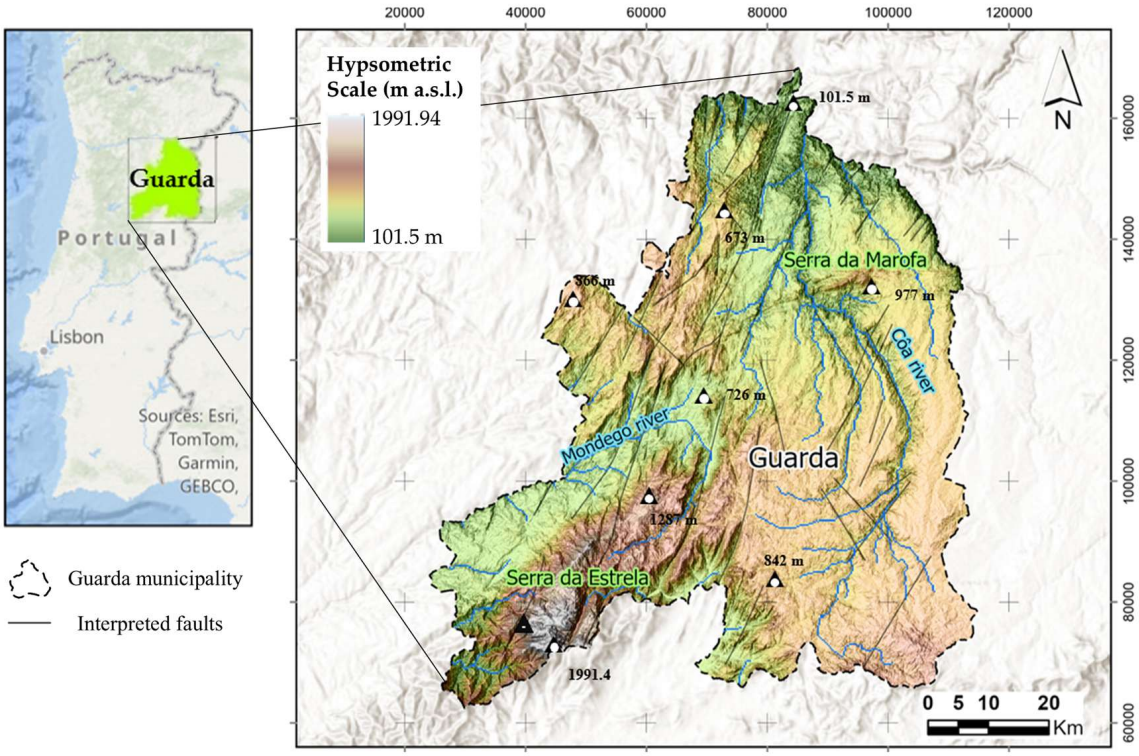

Figure 2. Geographic and geomorphological context of the Guarda District, Central Portugal.

3.2. Geological, Structural and Hydrogeothermal Setting

The Guarda District lies within the Central Iberian Zone of the Hesperian Massif and is dominated by Hercynian granitic rocks, locally associated with metasedimentary units of the Schist–Greywacke Complex (Figure 3). This lithological setting favours fracture networks and secondary permeability, which are essential for deep groundwater circulation in crystalline terrains [76]. The regional structure is marked by late Hercynian and neotectonic

faults, mainly oriented NE–SW, NNW–SSE, NNE–SSW and WNW–ESE. These faults define the main fracture corridors and may control infiltration, deep circulation and hydrothermal upflow, particularly where fracture zones, shear corridors and lithological contacts enhance permeability within the granitic massif [2,26,76].

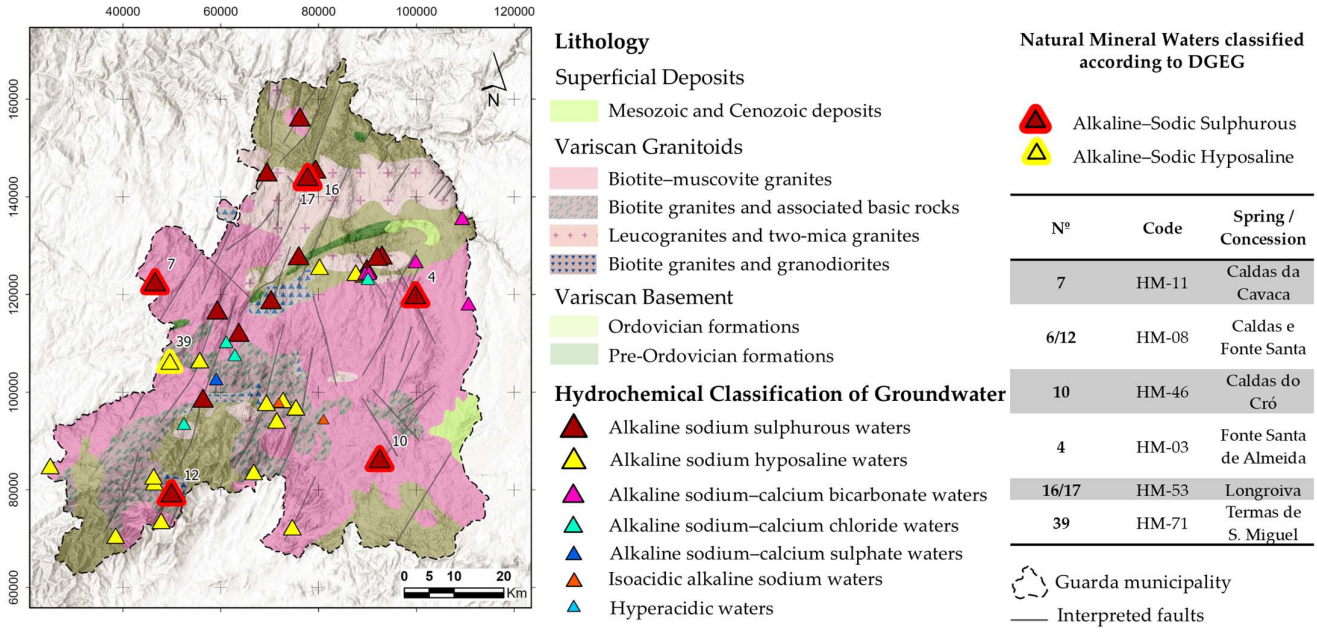

Nº	Code	Spring / Concession
7	HM-11	Caldas da Cavaca
6/12	HM-08	Caldas e Fonte Santa
10	HM-46	Caldas do Cró
4	HM-03	Fonte Santa de Almeida
16/17	HM-53	Longroiva
39	HM-71	Termas de S. Miguel

Figure 3. Geological and structural framework of the Guarda District, showing the main lithological units, mapped fault systems and special groundwater occurrences.

The Guarda District contains several special groundwater occurrences, a term used here to include both officially classified natural mineral waters and other groundwater occurrences with hydrochemical relevance to the regional hydrogeothermal framework. Among these, Longroiva is the only site officially classified as a geothermal resource, due to its approved exploitation plan for direct geothermal uses [18,32,77]. Longroiva, Cró, Almeida, Cavaca and Manteigas are commonly associated with major faults, structural intersections or granite–metasedimentary contacts, supporting a conceptual model of structurally controlled hydrothermal circulation [33,34]. Hydrogeochemically, sulphurous waters predominate among the analysed occurrences, followed by hyposaline and alkaline sodium–calcium waters, generally with low to moderate mineralisation and dissolved silica contents compatible with water–rock interaction in granitic environments [33]. In these fissured granitic and metasedimentary aquifers, groundwater flow, water–rock interaction and hydrothermal discharge are mainly governed by the connectivity of faults, fracture corridors, shear zones and lithological contacts [2,76–80]. Similar processes have also been reported in crystalline settings of Central and Northern Portugal [80–82]. Table 2 summarises the main classified natural mineral waters in the Guarda District, including estimated circulation depth, apparent silica-derived Tr indicator and geological–hydrogeological context [33,34].

Groundwater recharge varies markedly across the Douro, Mondego and Tejo river basins (Figure 4a), ranging from approximately 71 L/m^2/year in the Douro basin to 218 L/m^2/year in the Tejo basin. Higher recharge occurs mainly in the Mondego and Tejo sectors, where elevation and terrain dissection may favour infiltration. Unit discharge ranges from 0.04 L/s in the Douro basin to 0.11 L/s in the Mondego basin (Figure 4b), suggesting spatial differences in groundwater availability and potential subsurface flow paths relevant to hydrothermal discharge.

Table 2. Main classified natural mineral waters in the Guarda District, with estimated circulation depth, apparent silica-derived Tr indicator and geological–hydrogeological context, adapted from DGEG [34] and Marcos [33].

Location	Dr (km)	Tr (°C)	Geological-Hydrogeological Context
Caldas da Cavaca	~2.00	~101.04	Fractured granite; emergence close to fault intersection
Caldas e Fonte Santa—Manteigas	~1.10	~73.06	Fractured porphyritic granite; structurally influenced by the Manteigas fault
Caldas do Cró	~2.00	~99.51	Fractured granite; NNE–SSW and W–E tectonic node
Fonte Santa de Almeida	~1.45	~73.06	Coarse porphyritic granite; structurally associated with the Côa River fault
Termas de S. Miguel	~1.05	~70.73	Porphyritic biotite granite; semi-confined aquifer system
Termas de Longroiva	~1.9	~109.34	Highly fractured granite; artesianism related to schist–granite fault contact

Dr—estimated circulation depth; Tr—apparent silica-derived indicator.

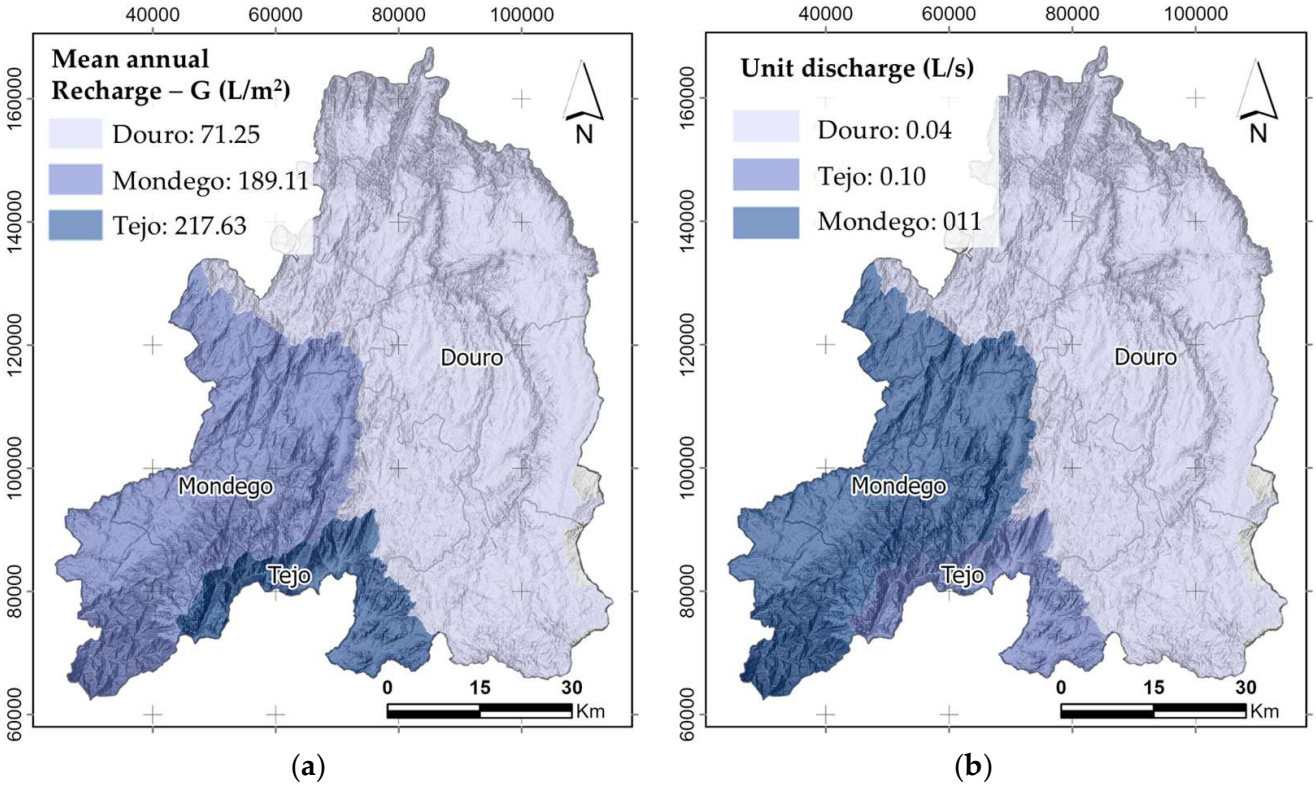

Figure 4. Spatial distribution of the Douro, Mondego and Tejo river basins in the Guarda District, showing: (**a**) mean annual groundwater recharge, expressed in L/m^2/year; and (**b**) unit discharge, expressed in L/s.

4. Materials and Methods

4.1. Dataset and Methodological Workflow

This study uses hydrogeochemical data from 54 special groundwater abstraction points in the Guarda District [33], covering fractured Hercynian granites, granite–metasedimentary contacts, mapped fault zones, mountain recharge areas, plateau surfaces, structural valleys and lower-elevation discharge sectors. Although spatially irregular, the dataset captures the main lithological, structural and geomorphological settings relevant to a screening-level geothermal assessment. Apparent silica-derived temperature indicators,

circulation depth, geothermal gradient and theoretical thermal power were estimated and integrated in a GIS environment using Empirical Bayesian Kriging Regression Prediction (EBKRP), with distance to major mapped faults as the structural covariate for the preliminary geothermal favourability map (Figure 5). The methodological workflow included the following steps:

(i) Compilation and standardisation of the groundwater dataset;
(ii) Estimation of apparent silica-derived temperature using silica geothermometers;
(iii) Calculation of circulation depth and geothermal gradient using classical hydrothermal relationships;
(iv) Estimation of theoretical thermal power;
(v) Calculation of distance to major mapped fault systems;
(vi) Spatial modelling using EBKRP; and
(vii) Validation and interpretation of the resulting geothermal favourability map.

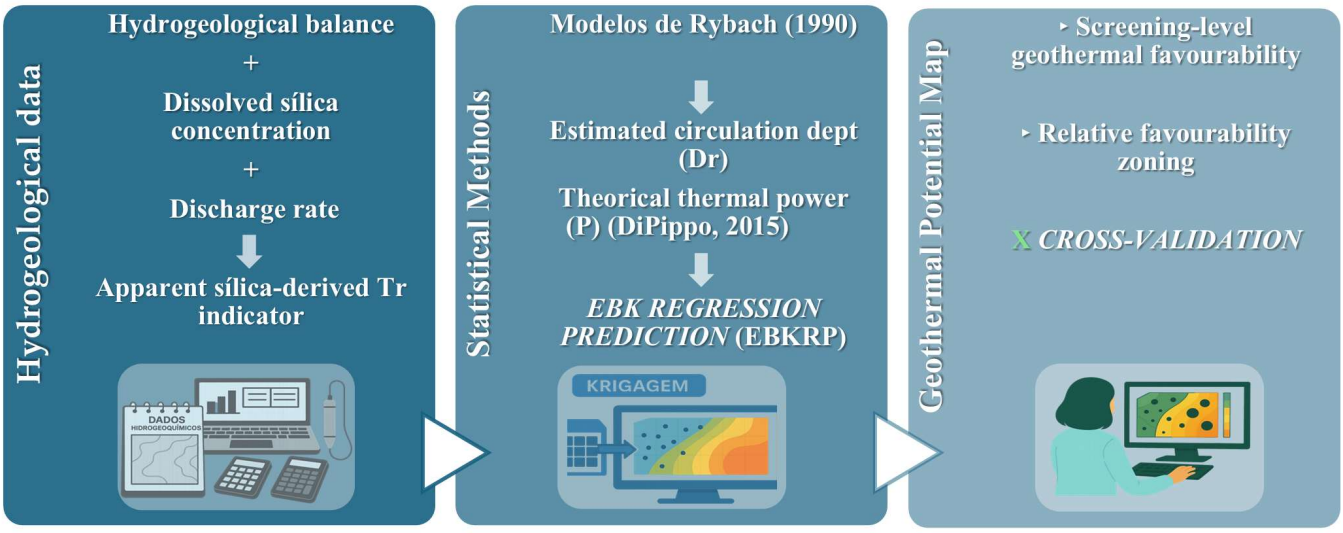

Figure 5. Methodological workflow adopted for the exploratory GIS-based geothermal favourability assessment of the Guarda District [15,83].

4.2. Silica Geothermometry and Hydrothermal Parameters

The apparent silica-derived temperature indicator, Tr, was calculated from dissolved silica concentration, C (mg/L), using the classical silica geothermometric equations [58,81], as systematised by Ferreira Gomes (2015) [77] (Table 3). This methodological choice follows previous hydrogeothermal studies in the Guarda District and in comparable Portuguese sulphurous waters hosted by Hercynian granitic fractured systems, where silica-based equations provided the most convergent and stable temperature estimates [33,77]. The approach was retained to ensure comparability with the regional Portuguese hydrogeothermal literature, particularly studies developed in Hercynian granitic and sulphurous-water systems. This methodological choice is also consistent with the Portuguese hydrogeothermal literature on granitic massifs, where quartz conductive and adiabatic silica geothermometers have been used as regional comparative indicators in meteoric-water systems circulating through fractured Hercynian granites [60–63,84,85]. Previous studies have also shown that, in granitic terrains, dissolved silica may be influenced by water–rock interactions with silicate minerals and not exclusively by equilibrium with a single silica polymorph [62,84–87].

Amorphous silica geothermometer controls may be more appropriate in some low-temperature groundwater systems [64]. However, because the present work aims at regional comparison with previous Portuguese studies conducted in fractured Hercynian

granitic terrains, and because the available dataset does not allow rigorous equilibrium assessment for each sampled water, the quartz-based formulations were retained as a consistent comparative framework. Their outputs are therefore interpreted exclusively as apparent hydrogeochemical indicators and not as equilibrium reservoir temperatures.

Table 3. Silica geothermometric equations retained from the regional Portuguese reference methodology and used in this study to derive apparent silica-derived temperature indicators.

Geothermometer	Equation	Limitation	Author
Conductive Quartz	$Tr = 1309/(5.19 - \log C) - 273.15$	0–250 °C	[85]
(Silica)	$Tr = 1164/(4.9 - \log C) - 273.15$	25–180 °C	[58]
Adiabatic Quartz (Silica)	$Tr = 1522/(5.75 - \log C) - 273.15$	0–250 °C	[85]
(Silica)	$Tr = 1498/(5.7 - \log C) - 273.15$	25–180 °C	[58]

Note: The terms quartz and silica refer to the original nomenclature of the equations reported in the cited sources. In this study, these formulations are not used to infer quartz–water equilibrium or absolute reservoir temperature. Considering the possible role of chalcedony or amorphous silica at lower temperatures, the resulting Tr values are interpreted only as apparent, comparative, screening-level hydrogeochemical indicators.

The quartz geothermometric equations are therefore not used here to demonstrate thermodynamic equilibrium with quartz, nor to provide absolute reservoir-temperature estimates. Instead, the calculated Tr values are interpreted as apparent and comparative hydrogeochemical indicators for regional geothermal screening. This interpretation explicitly acknowledges that, in low-temperature systems, dissolved silica may be influenced by chalcedony or amorphous silica control, as well as by cooling, mixing and incomplete re-equilibration during fluid ascent. Therefore, the selection of the silica equations adopted in this study is based not solely on general temperature thresholds but also on comparability with previous Portuguese hydrogeothermal studies developed in fractured Hercynian granitic and sulphurous-water systems. This cautious interpretation is consistent with general geothermometric guidance for low-temperature geothermal systems, while preserving comparability with the regional Portuguese reference methodology.

Circulation depth and geothermal gradient were estimated using the classical approach of Rybach (1990) [83], applied here to the apparent silica-derived temperature indicator, discharge temperature and geothermal gradient.

$$T_i = T_0 + G \times P_i \quad (1)$$

where T_i is the temperature at depth P_i, T_0 is the local discharge or near-surface reference temperature, and G is the geothermal gradient. This relationship was applied to each analysed point to estimate circulation depth and geothermal gradient, enabling regional comparison of hydrothermal circulation patterns across the Guarda District.

4.3. Theoretical Thermal Power Calculation

The theoretical available thermal power was calculated using the classical geothermal engineering expression [15]:

$$P = Q \times \rho \times C_p \times (T_r - T_E) \quad (2)$$

where P is the theoretical thermal power, expressed in W; ρ is the density of water; C_p is the specific heat capacity of water; Q is the discharge rate, expressed in m^3/s; T_r is the apparent silica-derived temperature indicator, expressed in °C; and T_E is the adopted reference temperature, expressed in °C. In this study, standard values of $\rho = 1000$ kg m^{-3} and $C_p = 4186$ J kg^{-1} $°C^{-1}$ were adopted.

A basin-specific reference temperature, T_E, was assigned to each abstraction point according to its location within the Douro, Mondego or Tejo river basin. These values,

obtained from the hydrogeological dataset [33], range from 9.51 °C to 11.51 °C and were used to calculate the temperature difference between the apparent silica-derived temperature indicator, Tr, and the reference condition. Discharge values from the same dataset, originally reported in L/s, were converted to m^3/s before estimating theoretical thermal power. These values are treated as standardised inputs for preliminary assessment, not as validated sustainable production rates; therefore, uncertainty in Q propagates directly into the calculated thermal-power values and was considered when interpreting the spatial favourability model.

4.4. EBKRP Spatial Modelling and Fault-Distance Covariate

Spatial modelling was performed in ArcGIS Pro 3.4 using Empirical Bayesian Kriging Regression Prediction (EBKRP), following Gribov and Krivoruchko (2020) [72] and Krivoruchko and Gribov (2019) [73]. EBKRP combines regression and Empirical Bayesian Kriging, allowing explanatory covariates and prediction uncertainty to be incorporated into the model. The logarithm of theoretical thermal power, $\log_{10}(P)$, was used as the dependent variable to reduce distribution skewness, while distance to major mapped faults was adopted as the structural covariate. A 1000 m fault-proximity buffer was used as a regional screening criterion, considering the study scale, fault-mapping uncertainty and the expected influence of fault-related fracture networks on secondary permeability. As other variables were not available with homogeneous spatial coverage, the resulting map is interpreted as a preliminary favourability model, not as a definitive quantification of geothermal resources.

5. Results

5.1. Apparent Silica-Derived Temperature Indicators and Geothermal Gradient

Silica-derived apparent geothermometric indicators mostly fall within the low- to medium-enthalpy range and should be interpreted as indicative estimates rather than direct reservoir measurements, as discussed in Section 4.2. Apparent silica-derived temperature indicators range from 21.3 °C to 121.2 °C, with a mean of 64.6 °C, showing marked spatial heterogeneity across the Guarda District (Figure 6a). The highest values, including local estimates above 100 °C, occur mainly in the Aguiar da Beira, Fornos de Algodres, Mêda, Trancoso, Pinhel, Figueira de Castelo Rodrigo and Almeida sectors.

Estimated geothermal gradients range from 20.3 °C/km to 92.1 °C/km, with a mean of approximately 45 °C/km (Figure 6b). Values between 40 and 65 °C/km are frequent, and local gradients above 65 °C/km occur particularly in the Manteigas sector and some central-eastern occurrences. The comparison between *T*r and *G* shows a generally coherent but non-uniform pattern, indicating that the estimated hydrogeothermal signal is influenced not only by the thermal gradient, but also by circulation depth, discharge conditions and structurally controlled groundwater flow.

5.2. Theoretical Thermal Power and EBKRP Geothermal Favourability Mapping

Theoretical thermal power, calculated from discharge rate and thermal differential using Equation (2), shows marked spatial variability across the Guarda District (Figure 7). Lower values are associated with low discharge rates and moderate apparent silica-derived Tr indicators, whereas the highest values, locally exceeding 1 MW, occur mainly in Aguiar da Beira, Fornos de Algodres, Mêda, Manteigas and Almeida, broadly following NE–SW and NNW–SSE structural trends. The EBKRP model, applied to $\log_{10}$(P) with fault distance as the structural covariate, identifies higher geothermal favourability near the main fault systems and lower favourability where both thermal power and *T*r are reduced. The 1000 m fault-proximity buffer is used only as a regional screening criterion, not as

a physical boundary of hydrothermal circulation; areas outside this buffer may still be relevant where unmapped fractures, secondary fault branches or lithological contacts enhance groundwater flow.

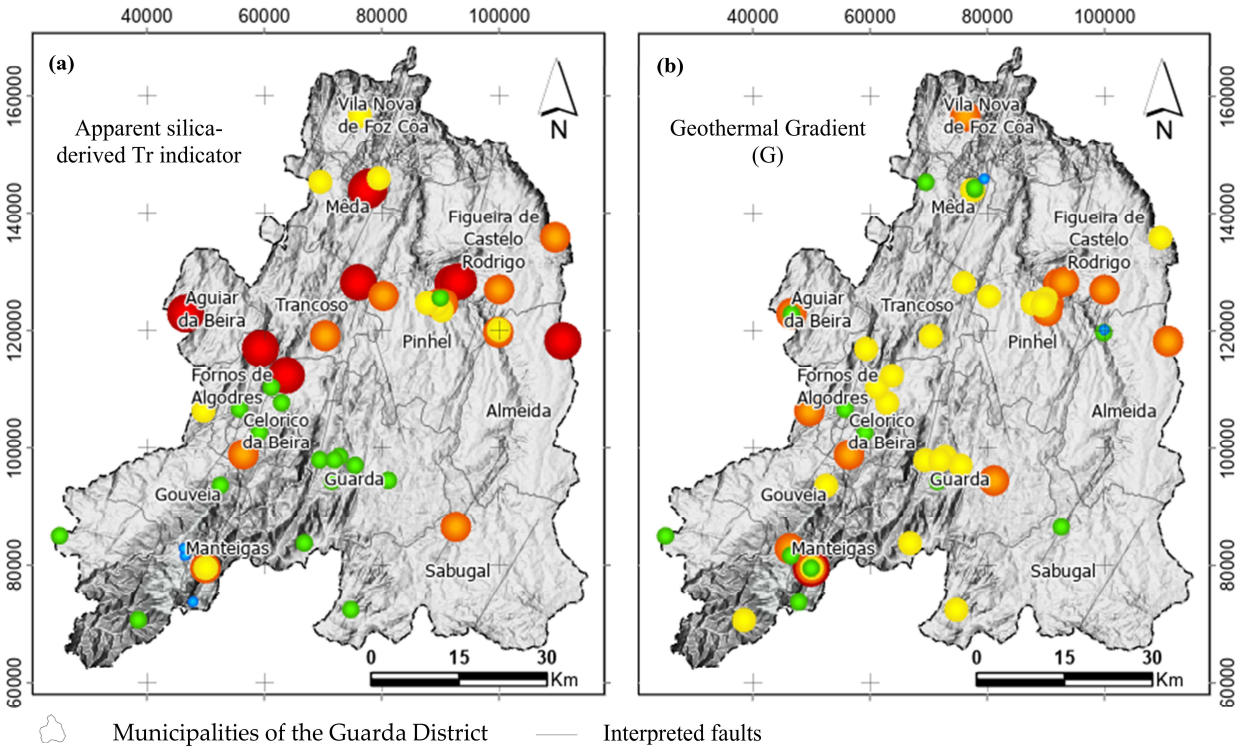

Geothermal classification of Apparent silica-derived Tr indicator and geothermal gradient

	Apparent silica-derived Tr indicator (°C)	Geothermal gradient (°C/km)
●	20–37: Low temperature	20–30: Background gradient
●	37–64: Moderate temperature	30–40: Slightly elevated
●	64–84: Elevated temperature	40–50: Moderately elevated
●	84–100: High temperature	50–65: High gradient
●	>100: Very high/anomalous	>65: Very high/anomalous

Figure 6. Spatial distribution of estimated hydrogeothermal indicators in the Guarda District: (**a**) apparent silica-derived temperature indicator, T_r (°C); and (**b**) estimated geothermal gradient, G (°C/km).

5.3. EBKRP Cross-Validation and Model Uncertainty

Leave-one-out cross-validation indicates acceptable internal performance for a preliminary regional EBKRP model based on indirect hydrogeothermal indicators, with a mean error close to zero (ME ≈ 0.062), RMSE of 0.497 in $\log_{10}$-transformed units, prediction-interval coverage of 92.3% and 98.1% for the 90% and 95% intervals, respectively, and a standardised RMS error of 0.829. These metrics suggest limited systematic bias and broadly consistent modelled uncertainty; however, the output remains constrained by the irregular distribution of sampling points, the indirect nature of silica geothermometry, discharge-rate uncertainty and the simplified representation of structural control through distance to mapped faults. Therefore, the EBKRP map should be interpreted as a comparative geothermal favourability product, rather than as definitive evidence of exploitable geothermal resources.

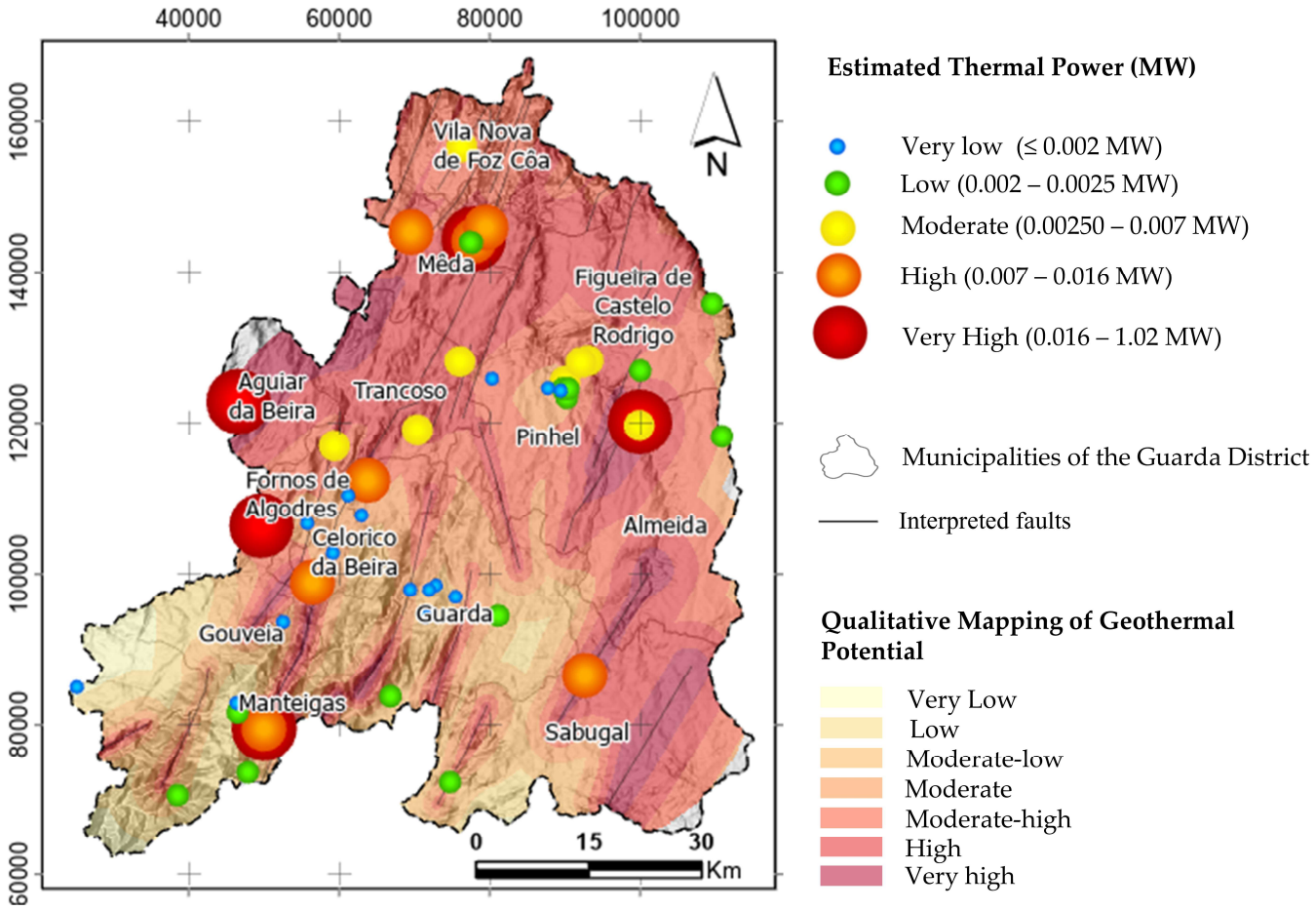

Figure 7. Spatial distribution of theoretical thermal power and EBKRP-derived geothermal favourability in the Guarda District.

6. Discussion

6.1. Hydrogeothermal Interpretation of Thermal Anomalies

Overall, the results indicate a heterogeneous low- to medium-enthalpy hydrogeothermal pattern in which the most favourable sectors likely reflect the combined influence of recharge conditions, circulation depth, residence time and structurally controlled permeability. Accordingly, the mapped anomalies should be interpreted as preliminary indicators of enhanced hydrothermal circulation, not as direct evidence of exploitable reservoir conditions.

Fault distance is a useful regional proxy for structural permeability, but it cannot represent fault connectivity, hydraulic behaviour or unmapped fracture networks. Therefore, the favourability map requires site-scale structural and geophysical validation.

6.2. Practical Implications for Regional Planning and International Comparison

Comparable fractured crystalline systems in Europe and Asia show that moderate to locally higher apparent silica-derived temperature indicators can occur where deep circulation is controlled by permeable fault systems [5–8]. In the Guarda District, this comparison supports the proposed conceptual model but does not replace direct subsurface validation.

The EBKRP-based map is intended as a regional screening tool to prioritise future structural, geophysical, drilling and hydrogeological investigations. It may guide the strategic sectors for future assessment of direct-use applications. Any consideration of electricity generation or binary-cycle systems remains outside the scope of the present

screening study and would require direct subsurface validation, sustainable flow-rate assessment, reinjection analysis, conversion-efficiency evaluation and techno-economic feasibility studies.

6.3. Limitations of the Study

The main limitation of this study is the absence of deep boreholes, borehole temperature logs and hydraulic test data, which prevents direct validation of reservoir conditions and recoverable thermal power. Uncertainty propagates through the workflow from silica-derived apparent geothermometric indicators, discharge-rate values and derived hydrothermal parameters to the EBKRP model and is further affected by irregular sampling and the simplified representation of structural control through fault distance. Although cross-validation supports the internal consistency of the EBKRP output, the map remains an exploratory screening product, not evidence of exploitable reservoirs or recoverable reserves [83,87–89]. Future work should include geochemical modelling, saturation analysis, direct temperature measurements, hydraulic testing, geophysical surveys, sensitivity analysis and, where relevant, seismological monitoring.

An additional source of uncertainty arises from the selection of the silica phase controlling dissolved silica concentrations. Depending on local hydrogeochemical conditions, chalcedony or amorphous silica may provide lower temperature estimates than quartz-based formulations. Because detailed equilibrium modelling was beyond the scope of this regional screening study, the adopted temperatures should be regarded as relative indicators rather than definitive estimates of subsurface thermal conditions. The present approach should therefore be understood as a regional hydrogeothermal screening method grounded in previous Portuguese studies, rather than as a thermodynamic equilibrium assessment of silica polymorphs at each sampling point.

7. Conclusions and Perspectives

This study developed an exploratory GIS-based approach to geothermal favourability mapping in the Guarda District, Central Portugal, integrating hydrogeochemical data from 54 special groundwater abstraction points, silica geothermometry, classical hydrothermal-parameter estimation and EBKRP spatial modelling. The main conclusions are as follows:

1. Apparent silica-derived temperature indicators range from 21.3 °C to 121.2 °C, with a mean value of 64.6 °C. These values indicate a predominantly low- to medium-enthalpy screening context and support the preliminary identification of sectors potentially favourable for direct geothermal uses.
2. The interpretation of the silica-derived temperature indicators explicitly considers the uncertainty associated with silica polymorph selection, including possible chalcedony or amorphous silica control at lower temperatures, as well as cooling, mixing and incomplete re-equilibration during fluid ascent. Consequently, the reported temperatures are interpreted only as apparent hydrogeochemical indicators for comparative regional assessment and not as direct reservoir-temperature estimates or definitive evidence of quartz–water equilibrium.
3. Estimated geothermal gradients range from 20.3 °C/km to 92.1 °C/km, with several sectors exceeding the average continental crustal gradient, suggesting spatially variable hydrothermal conditions across the district.
4. Higher apparent silica-derived temperature indicators, geothermal gradients and theoretical thermal-power values occur preferentially near major NE–SW and NNW–SSE fault systems, suggesting a possible influence of structurally controlled permeability in deep groundwater circulation within fractured Hercynian granitic terrains.

5. The EBKRP model, using $\log_{10}(P)$ as the dependent variable and distance to major mapped faults as the structural covariate, enabled the production of a preliminary geothermal favourability map. This map should be interpreted as a comparative screening product, not as a direct quantification of recoverable geothermal reserves or confirmation of exploitable reservoirs.
6. The results remain constrained by the absence of direct subsurface validation, irregular sampling, indirect geothermometric estimation, discharge-rate uncertainty and the simplified representation of structural control. Future work should include borehole temperature logging, exploratory drilling, hydraulic testing, geochemical modelling, mineral saturation analysis, geophysical surveys and sensitivity analysis to validate the most favourable sectors and assess their technical and economic feasibility.

Author Contributions: V.G. [Conceptualization, Data Curation, Methodology, Formal Analysis, Investigation, Writing—original draft preparation, Software, Validation]; L.M. [Methodology, Formal Analysis, Writing—review and editing, Validation]; M.V.M. [Methodology, Formal Analysis, Writing—review and editing, Validation]; L.M.F.G. [Conceptualization, Data Curation, Investigation, Writing—review and editing, Resources]; A.A. [Conceptualization, Writing—review and editing, Resources, Supervision]; P.G.A. [Conceptualization, Writing—review and editing, Software, Validation]; H.A.S.P. [Methodology, Writing—review and editing, Investigation, Validation]; L.J.A.P. [Methodology, Writing—review and editing, Investigation, Validation]. All authors have read and agreed to the published version of the manuscript.

Funding: This research received no external funding.

Data Availability Statement: All data available are in this paper.

Acknowledgments: The authors acknowledge the support from the GeoBioTec Research Unit through strategic projects (UID/04035/2025; https://doi.org/10.54499/UID/04035/2025) funded by the Fundação para a Ciência e a Tecnologia, IP/MCTES, through national funds (PIDDAC) for the period 2025–2029.

Conflicts of Interest: The authors declare no conflicts of interest.

References

1. Fridleifsson, I.B. Geothermal Energy for the Benefit of the People. *Renew. Sustain. Energy Rev.* **2001**, *5*, 299–312. [CrossRef]
2. Ferreira Gomes, L.M.; Andrade Pais, L.; Mendes, E. Contribution for the Knowledge of the Fracturing and Hydraulic Characterization of the Granitic Pluton of Castro Daire Region Viseu (Portugal). In Proceedings of the 11th ISRM Congress, Lisbon, Portugal, 9–13 July 2007.
3. Glaas, C.; Vidal, J.; Genter, A. Structural Characterization of Naturally Fractured Geothermal Reservoirs in the Central Upper Rhine Graben. *J. Struct. Geol.* **2021**, *148*, 104370. [CrossRef]
4. Frey, M.; Bossennec, C.; Seib, L.; Bär, K.; Schill, E.; Sass, I. Interdisciplinary Fracture Network Characterization in the Crystalline Basement: A Case Study from the Southern Odenwald, SW Germany. *Solid Earth* **2022**, *13*, 935–955. [CrossRef]
5. Zhou, C.; Liu, G.; Liao, S. Probing Fractured Reservoir of Enhanced Geothermal Systems with Fuzzy-Genetic Inversion Model: Impacts of Geothermal Reservoir Environment. *Energy* **2024**, *290*, 130320. [CrossRef]
6. Lu, Y.-C.; Song, S.-R.; Song, T.-J.; Wang, C.; Lin, A.T.-S.; Taguchi, S. Applicability of Na/K Geothermometer to the Metapelitic Non-Volcanic Geothermal Fields in the Taiwan Orogenic Belt. *Geothermics* **2024**, *124*, 103133. [CrossRef]
7. Genter, A.; Evans, K.; Cuenot, N.; Fritsch, D.; Sanjuan, B. Contribution of the Exploration of Deep Crystalline Fractured Reservoir of Soultz to the Knowledge of Enhanced Geothermal Systems (EGS). *Comptes Rendus Geosci.* **2009**, *342*, 502–516.
8. Stober, I.; Giovanoli, F.; Wiebe, V.; Bucher, K. Deep Hydrochemical Section through the Central Alps: Evolution of Deep Water in the Continental Upper Crust and Solute Acquisition during Water–Rock-Interaction along the Sedrun Section of the Gotthard Base Tunnel. *Swiss J. Geosci.* **2022**, *115*, 9. [CrossRef]
9. Bertani, R. Long-Term Projections of Geothermal-Electric Development in the World. In Proceedings of the Geo-THERM, Offenburg, Germany, 5–6 March 2009; pp. 5–6.
10. GEM. *Global Geothermal Power Tracker*; Global Energy Monitor: Covina, CA, USA, 2025.

11. Axelsson, G. The Future of Geothermal Energy. In *Living with Climate Change*; Elsevier: Amsterdam, The Netherlands, 2024; pp. 397–422.
12. Lund, J.W.; Toth, A.N. Direct Utilization of Geothermal Energy 2020 Worldwide Review. *Geothermics* **2021**, *90*, 101915. [CrossRef]
13. Çuhac, C.; Mäkiranta, A.; Välisuo, P.; Hiltunen, E.; Elmusrati, M. Temperature Measurements on a Solar and Low Enthalpy Geothermal Open-Air Asphalt Surface Platform in a Cold Climate Region. *Energies* **2020**, *13*, 979. [CrossRef]
14. Ferreira Gomes, L.M.; Trota, A.P.N.; de Albuquerque, F.J.R.A. Experience Gained on Direct Use of Low Enthalpy Energy in Hotel Do Parque, S. Pedro Do Sul, Portugal. *IOP Conf. Ser. Earth Environ. Sci.* **2017**, *95*, 022017. [CrossRef]
15. DiPippo, R. *Geothermal Power Plants: Principles, Applications, Case Studies and Environmental Impact*, 4th ed.; Elsevier: Amsterdam, The Netherlands, 2015.
16. Lund, J.W.; Freeston, D.H.; Boyd, T.L. Direct Utilization of Geothermal Energy 2010 Worldwide Review. *Geothermics* **2011**, *40*, 159–180. [CrossRef]
17. Líndal, B. Industrial and Other Applications of Geothermal Energy, Except Power Production and District Heating. In *Geothermal Energy: Review of Research and Development*; UNESCO: Paris, France, 1973; pp. 135–148.
18. Ferreira Gomes, L.M. As Águas Minerais Termais. Desafios Sobre as Suas Aplicações Para o Futuro. In *Proceedings of XV ENCEGM*; Ordem dos Engenheiros: Ponta Delgada, Portugal, 2005; pp. 187–205.
19. Licharz, H.; Rösmann, P.; Krommweh, M.S.; Mostafa, E.; Büscher, W. Energy Efficiency of a Heat Pump System: Case Study in Two Pig Houses. *Energies* **2020**, *13*, 662. [CrossRef]
20. World Bank. *Direct Utilization of Geothermal Resources*; World Bank Group: Washington, DC, USA, 2022.
21. Budiono, A.; Suyitno, S.; Rosyadi, I.; Faishal, A.; Ilyas, A.X. A Systematic Review of the Design and Heat Transfer Performance of Enhanced Closed-Loop Geothermal Systems. *Energies* **2022**, *15*, 742. [CrossRef]
22. Ferreira Gomes, L.M. Aproveitamento Geotérmico Em Cascata Em São Pedro Do Sul. *Bol. Minas* **2007**, *42*, 7–19.
23. Nunes, J.C. Geothermal Energy Use, Country Update for Portugal. In Proceedings of the European Geothermal Congress 2022, Berlin, Germany, 17–21 October 2022.
24. Rocha, S.S.P.G. Caracterização de Sistemas Hidrotermais de Baixa Entalpia Na Ribeira Grande, Ilha de S. Miguel, Açores. Master's Thesis, Universidade NOVA de Lisboa, Lisbon, Portugal, 2011.
25. Nunes, J.C. The Azores Archipelago: Islands of Geodiversity. In *Volcanic Tourist Destinations*; Springer: Berlin/Heidelberg, Germany, 2014.
26. Cabeças, R.; Carvalho, J.; Nunes, J. Portugal Country Geothermal Update 2010. In Proceedings of the World Geothermal Congress, Bali, Indonesia, 25–29 April 2010; pp. 25–29.
27. Cabral, J.M.; Marques, F.; Figueiredo, P.; Matias, L. Active Surface Faulting or Landsliding in the Lower Tagus Valley (Portugal)? A Solved Controversy Concerning the Vila Chã de Ourique Site. *J. Seismol.* **2010**, *15*, 215–234. [CrossRef]
28. DGEG. *Plano Estratégico Para a Geotermia*; DGEG: Lisbon, Portugal, 2025; p. 20.
29. Ferreira Gomes, L.M.; Jorge, A.I.S.T.; Gonçalves, L.F. O Aproveitamento Geotérmico Em São Pedro Do Sul: Experiência de Duas Décadas e Meia. *Bol. Minas* **2025**, *57*, 45–74.
30. Nogueiro, R. Aproveitamento Geotérmico de Chaves. In *Boletim de Minas—Edição Especial Geotermia*; DGEG: Lisbon, Portugal, 2004; Volume 57, pp. 33–44.
31. Albuquerque, F.J.R.A. Energia Geotérmica Em Edifícios—O Caso Do Hotel Do Parque No Campo Geotérmico e Hidromineral de São Pedro Do Sul. Master's Thesis, University Beira Interior, Covilhã, Portugal, 2011.
32. Ferreira, P.J.C. Modelação de Sistemas Geohidráulicos Profundos Associados a Fraturas Extensas da Região da Meda. Ph.D. Thesis, University Beira Interior, Covilhã, Portugal, 2023.
33. Marcos, T.M.S. Contribuição Para o Conhecimento do Potencial Geotérmico do Distrito da Guarda. Master's Thesis, University Beira Interior, Covilhã, Portugal, 2016.
34. DGEG. Hidrogenoma—Recursos Hidrominerais e Geotérmicos de Portugal. Available online: https://hidrogenoma.dgeg.gov.pt/ (accessed on 22 January 2026).
35. Duque, M.R. Geothermal Heat Flow by Conduction in Mainland Portugal. *Inżynieria Miner.* **2024**, *1*, 1–4. [CrossRef]
36. Portuguese Republic Diary. *Diário da República n.° 123/2019*; Série I de 2019-07-01; Portuguese Republic Diary: Lisbon, Portugal, 2024; pp. 3208–3299.
37. Portuguese Republic Diary. *Diário da República n.° 211/2024*; Série I de 2024-10-30; Portuguese Republic Diary: Lisbon, Portugal, 2024.
38. Galego, R. DGEG Obtém Primeiro Financiamento do Fundo de Modernização Para Projectos de Geotermia em Portugal. *Edifícios Energ.* **2025**. Available online: https://edificioseenergia.pt/noticias/dgeg-obtem-primeiro-financiamento-do-fundo-de-modernizacao-para-projectos-de-geotermia-em-portugal/ (accessed on 27 December 2025).
39. Dickson, M.H.; Fanelli, M. *Geothermal Energy: Utilization and Technology*; Renewable Energies Series; UNESCO: Paris, France, 2003.
40. Hochstein, M.P. Classification and Assessment of Geothermal Resources. In *Small Geothermal Resources: A Guide to Development and Utilization*; UNITAR: New York, NY, USA, 1990; pp. 31–57.

41. Brown, D.W. Hot Dry Rock Reservoir Engineering. *Bull. Geotherm. Resour. Counc.* **1990**, *19*, 89–93.
42. Ahmed, T.H. *Reservoir Engineering Handbook*, 3rd ed.; Elsevier/Gulf Professional: Burlington, MA, USA, 2006.
43. Chen, L.; Zhang, J.; Xu, L.; Chen, S.; Li, Q.; Sun, Y.; Li, J.; Zhao, X. A Study on the Geothermal Circulation System of Granite: An Example from the Lancang Area, Yunnan. *Geothermics* **2024**, *116*, 102853. [CrossRef]
44. Pérez-Estay, N.; Molina-Piernas, E.; Roquer, T.; Aravena, D.; Araya Vargas, J.; Morata, D.; Arancibia, G.; Valdenegro, P.; García, K.; Elizalde, D. Shallow Anatomy of Hydrothermal Systems Controlled by the Liquiñe-Ofqui Fault System and the Andean Transverse Faults: Geophysical Imaging of Fluid Pathways and Practical Implications for Geothermal Exploration. *Geothermics* **2022**, *104*, 102435. [CrossRef]
45. Roquer, T.; Arancibia, G.; Crempien, J.G.F.; Mery, D.; Rowland, J.; Sepúlveda, J.; Veloso, E.E.; Nehler, M.; Bracke, R.; Morata, D. Multi-Scale Flow Structure of a Strike-Slip Tectonic Setting: A Self-Similar Model for the Liquiñe-Ofqui Fault System and the Andean Transverse Faults, Southern Andes (39–40°S). *Geothermics* **2022**, *103*, 102424. [CrossRef]
46. Ferreira Gomes, L.M. Elementos Construtivos e Hidráulicos Da Nova Captação de Água Mineral Das Termas de Carvalhal—Castro Daire. *Bol. Minas* **2007**, *42*, 137–148.
47. Källberg, P.; Ferreira Gomes, L.M. Contribuição Para a Produção de Eletricidade em Portugal Continental a Partir de Aproveitamentos em Cascata. In *Seminário de Geotermia 2025—Energia Geotérmica em Portugal: Situação Atual e Desafios Para o Futuro—Livro de Atas*; Universidade da Beira Interior: Covilhã, Portugal, 2026; pp. 39–40.
48. Miranda, M.; Pires, R. Produção de Eletricidade a Partir de Recursos Geotérmicos de Baixa Temperatura em Portugal Continental: É Rentável? In *Seminário de Geotermia 2025—Energia Geotérmica em Portugal: Situação Atual e Desafios Para o Futuro—Livro de Atas*; UBI: Covilhã, Portugal, 2026; pp. 63–68.
49. Trota, A.; Ferreira, P.; Gomes, L.; Cabral, J.; Kallberg, P. Power Production Estimates from Geothermal Resources by Means of Small-Size Compact Climeon Heat Power Converters: Case Studies from Portugal (Sete Cidades, Azores and Longroiva Spa, Mainland). *Energies* **2019**, *12*, 2838. [CrossRef]
50. Armstead, H.C.H. *Geothermal Energy: Review of Research and Development*; Earth Sciences; UNESCO Publishing: Paris, France, 1973; Volume 12.
51. Wang, Y.; Zhang, X.; Qian, J.; Li, X.; Liu, Y.; Wu, W.; Lu, Z.; Xie, B. Machine and Deep Learning-Based Prediction of Potential Geothermal Areas in Hangjiahu Plain by Integrating Remote Sensing Data and GIS. *Energy* **2025**, *315*, 134370. [CrossRef]
52. Zhang, Y.; Zhang, Y.; Yu, H.; Li, J.; Xie, Y.; Lei, Z. Geothermal Resource Potential Assessment of Fujian Province, China, Based on Geographic Information System (GIS)-Supported Models. *Renew. Energy* **2020**, *153*, 564–579. [CrossRef]
53. Zhu, Z.; Lei, X.; Xu, N.; Shao, D.; Jiang, X.; Wu, X. Integration of 3D Geological Modeling and Geothermal Field Analysis for the Evaluation of Geothermal Reserves in the Northwest of Beijing Plain, China. *Water* **2020**, *12*, 638. [CrossRef]
54. Fournier, R.O. Chemical Geothermometers and Mixing Models for Geothermal Systems. *Geothermics* **1977**, *5*, 41–50. [CrossRef]
55. Giggenbach, W.F. Geothermal Solute Equilibria. Derivation of Na-K-Mg-Ca Geoindicators. *Geochim. Cosmochim. Acta* **1988**, *52*, 2749–2765. [CrossRef]
56. Nicholson, K. *Geothermal Fluids*, 1st ed.; Springer: Berlin/Heidelberg, Germany, 1993.
57. Spycher, N.; Peiffer, L.; Sonnenthal, E.L.; Saldi, G.; Reed, M.H.; Kennedy, B.M. Integrated Multicomponent Solute Geothermometry. *Geothermics* **2014**, *51*, 113–123. [CrossRef]
58. Arnórsson, S.; Gunnlaugsson, E.; Svavarsson, H. The Chemistry of Geothermal Waters in Iceland. III. Chemical Geothermometry in Geothermal Investigations. *Geochim. Cosmochim. Acta* **1983**, *47*, 567–577. [CrossRef]
59. Minissale, A.A. A Simple Geochemical Prospecting Method for Geothermal Resources in Flat Areas. *Geothermics* **2018**, *72*, 258–267. [CrossRef]
60. Aires de Barros, L. Termometria geoquímica. Princípios gerais, Aplicações Geotérmicas a casos portugueses. *Com. Serv. Geol. Port.* **1979**, *64*, 103–132.
61. Calado, C.M.A. A ocorrência de Água Sulfúrea Alcalina no Maciço Hespérico: Quadro Hidrogeológico e Quimiogénese. Ph.D. Thesis, University of Lisbon, Lisbon, Portugal, 2001; 462p.
62. Morais, M.J.F. Sistemas Hidrominerais nos Terrenos Graníticos da Zona Centro-Ibérica em Portugal Central: Perspectivas Químicas, Isotópicas e Genéticas Sobre as Águas Sulfúreas. Ph.D. Thesis, University of Coimbra, Coimbra, Portugal, 2013; 244p.
63. Ferreira Gomes, L.M.; Guedes, J.F.; Gomes da Costa, T.C.; Ferreira, P.J.C.; Trota, A.P.N. Geothermal potential of Portuguese granitic rock masses: Lessons learned from deep boreholes. *Environ. Earth Sci.* **2015**, *73*, 2963–2979. [CrossRef]
64. Arnórsson, S. *Isotopic and Chemical Techniques in Geothermal Exploration, Development and Use*; IAEA: Vienna, Austria, 2000.
65. Casasso, A.; Sethi, R. G.POT: A Quantitative Method for the Assessment and Mapping of the Shallow Geothermal Potential. *Energy* **2016**, *106*, 765–773. [CrossRef]
66. Li, X.; Huang, C.; Chen, W.; Li, Y.; Han, J.; Wang, X.; Bai, X.; Yin, Z.; Li, X.; Hou, P.; et al. GIS Model for Geothermal Advantageous Target Selection. *Sci. Rep.* **2023**, *13*, 6024. [CrossRef] [PubMed]

67. Łukawska, A.; Ryżyński, G.; Żeruń, M. Serial Laboratory Effective Thermal Conductivity Measurements of Cohesive and Non-Cohesive Soils for the Purpose of Shallow Geothermal Potential Mapping and Databases—Methodology and Testing Procedure Recommendations. *Energies* **2020**, *13*, 914. [CrossRef]
68. Perego, R.; Pera, S.; Galgaro, A. Techno-Economic Mapping for the Improvement of Shallow Geothermal Management in Southern Switzerland. *Energies* **2019**, *12*, 279. [CrossRef]
69. Malczewski, J. *GIS and Multicriteria Decision Analysis*; Wiley: Hoboken, NJ, USA, 1999.
70. Tende, A.W.; Miner Iiiya, M.; Habu, S.; Gajere, J.N.; Iyakwari, S.; Aminu, M.D. GIS-Based Multi-Criteria Predictive Modelling for Geothermal Energy Exploration. *Energy Geosci.* **2025**, *6*, 100409. [CrossRef]
71. Pratama, H.B.; Supijo, M.C.; Sutopo. Experimental Design and Response Surface Method in Geothermal Energy: A Comprehensive Study in Probabilistic Resource Assessment. *Geothermics* **2020**, *87*, 101869. [CrossRef]
72. Gribov, A.; Krivoruchko, K. Empirical Bayesian Kriging Implementation and Usage. *Sci. Total Environ.* **2020**, *722*, 137290. [CrossRef] [PubMed]
73. Krivoruchko, K.; Gribov, A. Evaluation of Empirical Bayesian Kriging. *Spat. Stat.* **2019**, *32*, 100368. [CrossRef]
74. Zaresefat, M.; Derakhshani, R.; Griffioen, J. Empirical Bayesian Kriging, a Robust Method for Spatial Data Interpolation of a Large Groundwater Quality Dataset from the Western Netherlands. *Water* **2024**, *16*, 2581. [CrossRef]
75. Haas, L.D.; Rehwald, M.J.; Hart, D.J.; Calkins, C.A. *Supplemental Report on Depth to Silurian Bedrock in Eastern Wisconsin*; Wisconsin Geological and Natural History Survey: Madison, WI, USA, 2025.
76. Ferreira, N.; Iglesias, M.; Noronha, F.; Pereira, E.; Ribeiro, A.; Ribeiro, M.L. Granitoides Da Zona Centro Ibérica e Seu Enquadramento Geodinâmico. Granitoides da Zona Centro Ibérica e seu Enquadramento Geodinâmico. In *Geología de los Granitorides y Rocas Asociadas del Macizo Hepérico Libro Homenaje a L.C. García de Figuerola.*; Rueda: Madrid, Spain, 1987; pp. 37–51.
77. Ferreira Gomes, L.M. Controlo de Qualidade Do Recurso Das Termas de Longroiva. *Boletín Soc. Española Hidrol. Médica* **2015**, *30*, 181–192. [CrossRef]
78. Almeida, C.; Lopo, M.; Jesus, M.; Gomes, A. *Sistemas Aquíferos de Portugal Continental*; Centro de Geologia da Universidade de Lisboa: Lisbon, Portugal; Instituto Nacional da Água: Buenos Aires, Argentina, 2000; Volume I.
79. Almeida, C.; Lopo, M.; Jesus, M.; Gomes, A. *Sistemas Aquíferos de Portugal Continental*; Centro de Geologia da Universidade de Lisboa: Lisbon, Portugal; Instituto Nacional da Água: Buenos Aires, Argentina, 2000; Volume II.
80. Almeida, C.; Lopo, M.; Jesus, M.; Gomes, A. *Sistemas Aquíferos de Portugal Continental*; Centro de Geologia da Universidade de Lisboa: Lisbon, Portugal; Instituto Nacional da Água: Buenos Aires, Argentina, 2000; Volume III.
81. Pacheco, F.; Van Der Weijden, C.H. Contributions of Water-Rock Interactions to the Composition of Groundwater in Areas with a Sizeable Anthropogenic Input: A Case Study of the Waters of the Fundão Area, Central Portugal. *Water Resour. Res.* **1996**, *32*, 3553–3570. [CrossRef]
82. Antunes, I.M.H.R.; Gonçalves, L.M.B. Hydrogeochemistry of an Ancient Groundwater System (Sete Fontes, Braga, Northern Portugal). In *Proceedings of SCTV-II*; Campus da Auga: Ourense, Spain, 2017.
83. Rybach, L. Determination of Thermal Water Circulation Depth, with Examples from the Valaisan Alps, Switzerland. In *Proceedings of the 22nd Congress of IAH*; IAH: Reading, UK, 1990; Volume 22, pp. 608–615.
84. Ferreira Gomes, L.M.; Antunes, I.M.H.R.; Albuquerque, M.T.D.; Santos Silva, A.J. New Thermal Mineral Water from Águas (Penamacor, Central Portugal): Hydrogeochemistry and Therapeutic Indications. *IOP Conf. Ser. Earth Environ. Sci.* **2019**, *221*, 012025. [CrossRef]
85. Fournier, R.O. Application of Water Geochemistry to Geothermal Exploration and Reservoir Engineering. In *Geothermal Systems: Principles and Case Histories*; John Wiley & Sons: New York, NY, USA, 1981.
86. Arnórsson, S. Application of the silica geothermometer in low temperature hydro-thermal areas in Iceland. *Amer. J. Sci.* **1975**, *275*, 763–784.
87. Arnórsson, S. Chemical equilibria in Icelandic geothermal systems. Implications for chemical geothermometry investigations. *Geothermics* **1983**, *12*, 119–128. [CrossRef]
88. Ferreira Gomes, L.; Madureira, P.; Figueira, J.; Pinto, C.; Pinto, H.; Ferreira, P. *Seminário de Geotermia 2025—Energia Geotérmica em Portugal: Situação Atual e Desafios para o Futuro*; UBI Edições: Covilhã, Portugal, 2025. [CrossRef]
89. Martínez-Garzón, P.; Zaliapin, I.V.; Ben-Zion, Y.; Kwiatek, G.; Bohnhoff, M. Comparative Study of Earthquake Clustering in Relation to Hydraulic Activities at Geothermal Fields in California. *JGR Solid Earth* **2018**, *123*, 4041–4062. [CrossRef]